

LOCALIZATION OF A WEAK REGION IN THE  
OLD NEUTRINO SHIELDING

by

L. Cucančić, H. Faissner, F. Ferrero,  
A. Ghani, E. Heer, F. Krienen, T.B. Novey,  
M. Reinharz and R.A. Salmeron.

SUMMARY

The muon background in the neutrino block-house was studied in detail, using telescopes of large liquid scintillation counters, registering the arrival time of muons relative to the PS bunch phase and scanning the flux by means of moveable plastic counters. The counter measurements were substantiated by observing the muon tracks in large area spark chambers. The muons were found to penetrate through the concrete shielding adjacent to the ring side of the central iron plug. Strengthening parts of this weak region by 2.4 m of iron reduced the intensity of the most directional muons by a factor of 4.

Geneva - August 1962.

LOCALIZATION OF A WEAK REGION IN THE  
OLD NEUTRINO SHIELDING

by

L. Cucančić, H. Faissner, F. Ferrero,  
A. Ghani, E. Heer, F. Krienen, T.B. Novey,  
M. Reinharz and R.A. Salmeron.

\* \* \*

1. INTRODUCTION

Our background measurements have been made in the following three runs:

	<u>Date</u>	<u>No. Shifts</u>	<u>Techniques Employed</u>
Run 1	July 61	10	liquid counters and time-of-flight
Run 2	August 61	1	liquid counters
Run 3	December 61	2	liquid counters, plastic counters and spark chambers.

Run 1 was done together with the Wilson chamber, and with the CERN and the EP bubble chambers, running in parallel. On this run only one or two shifts have been used for the detailed study of the charged background. More shielding was piled up in front of a suspected weak region for run 2 and 3.

In section 2 results are given of the time-of-flight measurements by which it was established that the charged background particles were coming along a trajectory not too different from the line-of-sight to the PS-target. The liquid counter measurements are described in section 3. A comparison of these

measurements, which were made in all the three runs, allowed us to estimate the effectiveness of the additional shielding. In sections 4 and 5 our measurements made with plastic counters and spark chambers are described.

## 2. TIME-OF-FLIGHT

The time-of-arrival of background particles with respect to the phase of the proton bunches was measured in run 1. For a description of the method see Ref. 1. The results are plotted in Fig. 1 together with a calibration measurement made at a PS energy of 27 GeV where muons can penetrate along the  $6^\circ$  line (cut-off 20.5 GeV muon energy). A measurement of the cosmic-ray background is included as well, showing, as can be expected a flat distribution.

The width of the peak observed at 24 GeV corresponds well to the length of the circulating proton bunches<sup>1)</sup>. This shows that the background particles come in along a well defined trajectory. As demonstrated by the approximate equality of the respective peak positions, the trajectories at 24 and 27 GeV are approximately the same. If one attributes the  $\approx 2$  nsec earlier rise at 27 GeV to muons travelling along the  $6^\circ$ -line, one concludes that the background trajectory is on the average  $\approx 60$  cm longer than the line-of-sight. This corresponds to a maximum lateral deviation of  $\approx 4$  m which checks well with the muon flux measurements described below. In fact they show that muons created under small angles travers the neutrino shielding to the left of the iron plug in the region marked X, in Fig. 2. The shielding thickness is only 25 m of baryte 1.5 m to the left of the  $6^\circ$  line, which corresponds to a cut-off energy of 17.5 GeV and the multiple scattering of muons is sufficiently large (average scattering angle 50 mrad for 22.5 initial energy) in order to allow part of them to reach the detector area.

### 3. LIQUID COUNTER TELESCOPE

The set-up (Fig. 3) consisted of a front counter F of  $2.4 \times 4 \text{ m}^2$ , three back-counters Y and one mobile counter X of  $1 \times 1.8 \text{ m}^2$  each, and a directional Čerenkov counter C of  $2.4 \times 1.6 \text{ m}^2$ . In run 1 and 2 the total F-counter was used, in run 3 only the left half of the F-counter (left when looking towards the target). In run 3 the mobile counter, X, was used in coincidence with all or with one of the Y-counters in the back.

Our results are given in Tables, I, II and III. The values in Table I were obtained under shielding conditions described in Ref. 2 for run 4. The values of Table II were obtained after extending the concrete shielding inside the ring, as indicated in Fig. 2 and the values of Table II with some additional iron placed in front equally indicated in Fig. 2.

A comparison between Tables I, II and II shows the reduction of counting rates, obtained for all the measured counter combinations, by strengthening the shielding to the left of the  $6^\circ$  line. In this way, e.g. our most directional coincidences (Y, F)<sup>2</sup> were reduced by a factor of 4.

For better localization of the residual particle flux we have moved the X-counter in a plane normal to the  $6^\circ$  line and measured coincidences with one of the Y-counters in the back. The values obtained for different positions and machine energies are plotted in Fig. 4. The maxima obtained seem to be pointing in the direction of the weak spot.

The location of the intensity maximum seems to be energy dependent, moving away from the  $6^\circ$  line as the PS energy decreases. This behaviour is probably due to a combination of various causes as, for example, the initial energy distribution of the muons and varying amount of shielding provided by the EP bubble chamber in front.

The dependence of the particle flux on machine energy is plotted in Fig. 5. The particle flux is reduced by approximately a factor of ten when decreasing the machine energy by 3 GeV. At a PS energy of 20 GeV we are very near or already at cosmic-ray level. This behaviour was already observed in our previous background runs<sup>2)</sup>.

#### 4. FLUX MEASUREMENTS WITH PLASTIC COUNTERS

The arrangement of plastic counters is indicated in Fig. 3. An iron absorber, 2.5 cm thick, was placed between two scintillators ( $100 \times 40 \text{ cm}^2$ , 1 cm thick) in coincidence. The absorber thickness corresponds to an energy cut-off of 60 MeV.

The flux was scanned in a plane perpendicular to the  $6^\circ$  line, in the same way as in the liquid counter measurements (section 2). The results which are plotted in Fig. 6 look quite similar to Fig. 4 obtained with the liquid counter telescope. The same shifting of the maximum can also be observed. The counting rates given in Table IV are somewhat higher than those obtained with liquid counters (Table III) if one normalizes to the same counting area. This can however easily be explained by the larger solid angle acceptance<sup>\*)</sup>. The values of Table IV have also been plotted in Fig. 5 from which the same energy dependence can be observed as in the case of the liquid counters.

#### 5. OBSERVATIONS MADE WITH SPARK CHAMBERS

Several spark chambers were set up behind the Y-counters in run 3. The arrangement was centred on the  $6^\circ$  line and consisted of a 4 gap brass chamber, a 4 gap iron chamber and two 2 gap aluminium chambers. The plate thickness in all the chambers was 0.5 cm. A paraffin oil Čerenkov counter of the non-directional type, placed between the brass and the aluminium chambers provided the trigger (see Fig. 3).

---

\*) as well as by the <sup>lower</sup> ~~higher~~ effective energy cut-off.

The results are summarized in Table V. At 27 and 24 GeV nearly all the observed tracks are confined within an angle of  $\pm 30^\circ$  from the horizontal. Already at 21 GeV the angular distribution of the tracks becomes consistent with the cosmic-ray distribution. The tracks do not interact in the chambers and have no appreciable scattering showing that we have indeed been measuring essentially muons.

## 6. CONCLUSIONS

The present measurements confirm the results of the previous ones<sup>2)</sup>, namely that the intensity of background muons was much higher than anticipated, and that it varied strongly with CPS energy. Moreover, the weak spot was found through which the muons could penetrate. It was the concrete region between the central iron plug and the CPS ring.

The present measurements remove the apparent discrepancy between our early counter measurements<sup>2)</sup> and the findings of the Ecole Polytechnique bubble chamber group,<sup>3)</sup> who observed almost no muon background at all. The bubble chamber was still essentially in the shadow of the central plug.

Although our measurements are not directly applicable to the next stage of the neutrino experiment with the external target and the magnetic horn, they teach us several things:

1. One should avoid a central iron shield of small lateral extension, surrounded by concrete, because muons easily go around it\*).

---

\*) The same experience was made by the Columbia-Brookhaven group<sup>4)</sup>. Their iron shielding was meant to be good at AGS energies  $> 20$  GeV. They had the same trouble with the "0°-beam" as described in the present report, and on top of that serious difficulties with muons sneaking in on top and through the floor. As a result they were forced to run at 15 GeV, which was not essential for the one-or-two-neutrino question, but a serious drawback in the search for the intermediate boson.

2. It is dangerous to think of background as coming in straight lines from the target. In our case the dangerous muons, because of the deflection in the stray field, came from a virtual target shifted appreciably towards the inside of the ring.
3. At 24 GeV CPS energy a cut-off energy of 17.5 GeV, combined with a scattering around 80 mrad is by no means safe.
4. The background muons were concentrated around the medium plane, i.e. floor and roof were (relatively) safe.

From this one may draw the following practical conclusions:

1. Rather than having iron concentrated on the line-of-sight to the target with soft regions around, one should make a sandwich structure, where the iron covers a large solid angle and the concrete is behind it. This was also strongly recommended by Lindenbaum<sup>5)</sup>.
2. Virtual and parasitic targets, at positions quite different from the real target, can never be avoided. Consequently one has to shield against all regions which may conceivably act as targets, (which is an almost impossible task).
3. The only safe thing was to have a cut-off energy bigger than the foreseen CPS energy of 24 GeV in all directions. As this meets with technical difficulties, one should at least take care that for cut-offs < 20 GeV the conceivable trajectories involve scattering angles  $\gg$  100 mrad.
4. The virtual absence of floor and bottom muons is easily explained by the aperture limiting coils and magnet structures close to the target, which absorbed a large part of the pions before they were able to decay. As these structures will be absent with the external target, one has to provide a local shielding around the horn, i.e. a funnel which leaves only the desired decay cone of  $\pm$  40 mrad open.

The funnel should be flared to the outside such that the more distant parts of it are not seen from the target. This would depress the probability of forming parasitic targets appreciably.

Finally it should be emphasized that a shielding at the required level of safety can really not be calculated. The past experience with neutrino shieldings on both sides of the Atlantic has been far from being brilliant. With the  $2 \mu$  sec burst from the ejected beam the neutrino spark chamber<sup>6)</sup> will be paralysed if more than 1 muon per pulse transverse it. This is simply due to the fact that the sensitive time is of the order of  $1 \mu$ sec, and the well known "robbing effect" of non-coincident tracks would make the efficient observation of  $\nu$ -events impossible. (For compensation actual stray muons might easily look like  $\nu$ -events.) The only sound conclusion then is to play safe.

#### ACKNOWLEDGEMENTS

The authors are indebted to the PS machine group under the direction of P. Germain for their outstanding collaboration during the runs. They acknowledge in particular the excellent job done by Dr. Bonaudi and his staff with installation and shielding, by Mr. Kröwerath and his crew with the transport and by Dr. Sluygers with the targets. The support from Professors Bernardini and Preiswerk is gratefully acknowledged. We wish to thank our technicians Mr. Doughty and Mr. Jørgensen, and their helpers, who worked hard and efficiently.



TABLE I COUNTING RATES OF LIQUID COUNTERS IN RUN 1 \*

Rates per 1000 Bursts. Gate length 1.5 msec.

ENERGY	$(Y_C)^2$	$(Y_5C)^2$	$(Y_6C)^2$	$(Y_7C)^2$	$(Y_5F)^2$	$(Y_6F)^2$	$(Y_7F)^2$	$(Y_{FL})^2$	$(Y_{FR})^2$	$(C_{FL})^2$	$(C_{F4})^2$	$(C_{F5})^2$	$(C_{F6})^2$	$(Y_{F5.6})^2$	$(Y_{F4})^2$	$(Y_{F5})^2$	$(Y_{F6})^2$	
24 GeV	1010± 29	47± 135	525± 564	435± 50.7	12± 6.7	318± 43.6	1325 ±88.5	1880± 105	14± 3.6	236± 26	0	187± 25	15±7	2100 ±98	50± 14	1000 ±55	280± 30	
COSMICS	3.5± 0.07	1.5± 0.05	1.2± 0.06	1± 0.05	0.25 ±0.04	0.3± 0.04	0.08 ±0.02	/	0.65 ±0.04	/	/	/	/	0.65 ±0.04	/	/	/	/

\* The counter  $F_L$  consists of three counters  $F_4$ ,  $F_5$  and  $F_6$  mounted one on top of the other.  $(AB)^2$  means a double coincidence between the counters A and B.

TABLE II COUNTING RATE OF LIQUID COUNTERS IN RUN 2  
 Rates per 1000 Bursts. Gate length 1.5 msec

ENERGY	$(Y_C)^2$	$(Y_{5C})^2$	$(Y_{6C})^2$	$(Y_{7C})^2$	$(Y_5 F)^2$	$(Y_6 F)^2$	$(Y_7 F)^2$	$(Y_{FL})^2$	$(Y_{FR})^2$
24 GeV	$630 \pm 33.3$	$48 \pm 19.0$	$314 \pm 33.5$	$300 \pm 46.5$	$14 \pm 8.1$	$215 \pm 27.5$	$1280 \pm 95.8$	$1220 \pm 66.0$	$29 \pm 10$
COSMICS	$9.7 \pm 0.1$	$2.7 \pm 0.08$	$4.3 \pm 0.1$	$2.7 \pm 0.08$	$0.3 \pm 0.03$	$0.4 \pm 0.03$	$0.2 \pm 0.02$	$0.76 \pm 0.04$	$1.03 \pm 0.05$

TABLE III COUNTING RATES OF LIQUID COUNTERS IN RUN 3\*

Rates per 1000 Bursts. Gate length 1.5 msec.

ENERGY	$(Y_C)^2$	$(Y_5 C)^2$	$(Y_6 C)^2$	$(Y_7 C)^2$	$(Y_5 F_L)^2$	$(Y_6 F_L)^2$	$(Y_7 F_L)^2$	$(X_{0.5} Y)^2$	$(X_{1.0} Y)^2$	$(X_{1.5} Y)^2$	$(X_{2.0} Y)^2$	$(X_{2.5} Y)^2$	$(X_{3.5} Y)^2$	$(X_{2.0} Y)^2$	$(F_4 Y)^2$	$(F_5 Y)^2$	$(F_6 Y)^2$
27 GeV	4614 ± 79	1196 ± 66	1313 ± 72	1700 ± 116	130 ± 23	1283 ± 64	4400 ± 188	1530 ± 110	/	5220 ± 240	/	1018 ± 61	288 ± 53	/	/	/	/
24 GeV	302 ± 16	41± 15	108± 23	148± 13	6± 6	83± 20	297 ± 28	40± 15	93± 23	270± 40	510± 55	335 ± 43	0	470± 50	70± 20	180± 33	107± 25
21 GeV	56± 9	4± 2.6	22± 9	/	0	15± 7.4	/	/	/	4± 4	/	47± 9.4	/	/	/	/	/
20 GeV	21± 5	/	/	5± 2.3	/	/	3± 2	/	/	3±2	/	/	/	/	/	/	/
COSMICS	9±0.1	2.4± 0.7	5.5± 0.37	2± 0.07	0.17± 0.02	0.24± 0.02	0.14± 0.02	/	/	0.05± 0.007	/	/	/	/	/	/	/

\* The index given to the X-counter represents its distance from the 6°-line in meters

TABLE IV

Counting Rates of Plastic Counters  
(Rates Per 1000 Bursts - Gate Length 1.5 msec)

PS Energy/GeV	Coincidence Rate
27	1240 ± 160
24	240 ± 70
21	12 ± 2.6
Cosmics	18 ± 0.7

TABLE V

Spark Chamber Observations

PS Energy/GeV	Gate Length	Per cent of Tracks Inclined to the Horizontal	
		0 ± 30°	> ± 30°
27	1.5 ms	92%	8%
24	0.5 ms	85%	15%
21	1.5 ms	19%	81%
20	1.5 ms	16%	84%
Cosmics	-	17%	83%

References

- 1) L. Cucančić and H. Faissner, CERN Report, in preparation.
- 2) H. Faissner, F. Ferrero and M. Reinharz, NP Internal Report 61-11 (1961).
- 3) M.A. Lagarrigue et al., Report on the background measurements with the Ecole Polytechnique Bubble Chamber (1962) and private communication.
- 4) G. Danby, M.M. Gaillard, D. Goulianos, L.M. Lederman, N. Mistry, M. Schwartz and J. Steinberger, Phys.Rev.Letts. 3, 36 (1962), and private communication.
- 5) S.J. Lindenbaum, Memorandum to the CERN Directorate, unpublished, and private communication.
- 6) H. Faissner, F. Ferrero, A. Ghani, E. Heer, F. Krienen, G. Muratori, T.B. Novey, M. Reinharz and R.A. Salmeron, Proc. CERN Conf. High Energy Instrument. (1962), in course of publication.

Figure Captions

- Fig. 1 : Time-of-flight spectra of muons from target 5, of charged background and of cosmic rays.
- Fig. 2 : Shielding layout for runs 1, 2 and 3.  
Note: X is lower.
- Fig. 3 : Counter set up in the neutrino block-house. The plastic counter, counters X and N and the spark chamber have been added only for run 3.
- Fig. 4 : Directional dependence of background as measured with the liquid counter telescope (XY-coincidences).
- Fig. 5 : Energy dependence of  $\mu$  flux as delivered by a coincidence between counters Y and the C-counter. The curve obtained with the plastic counter has also been plotted.
- Fig. 6 : Lateral dependence of background as measured with plastic counters.

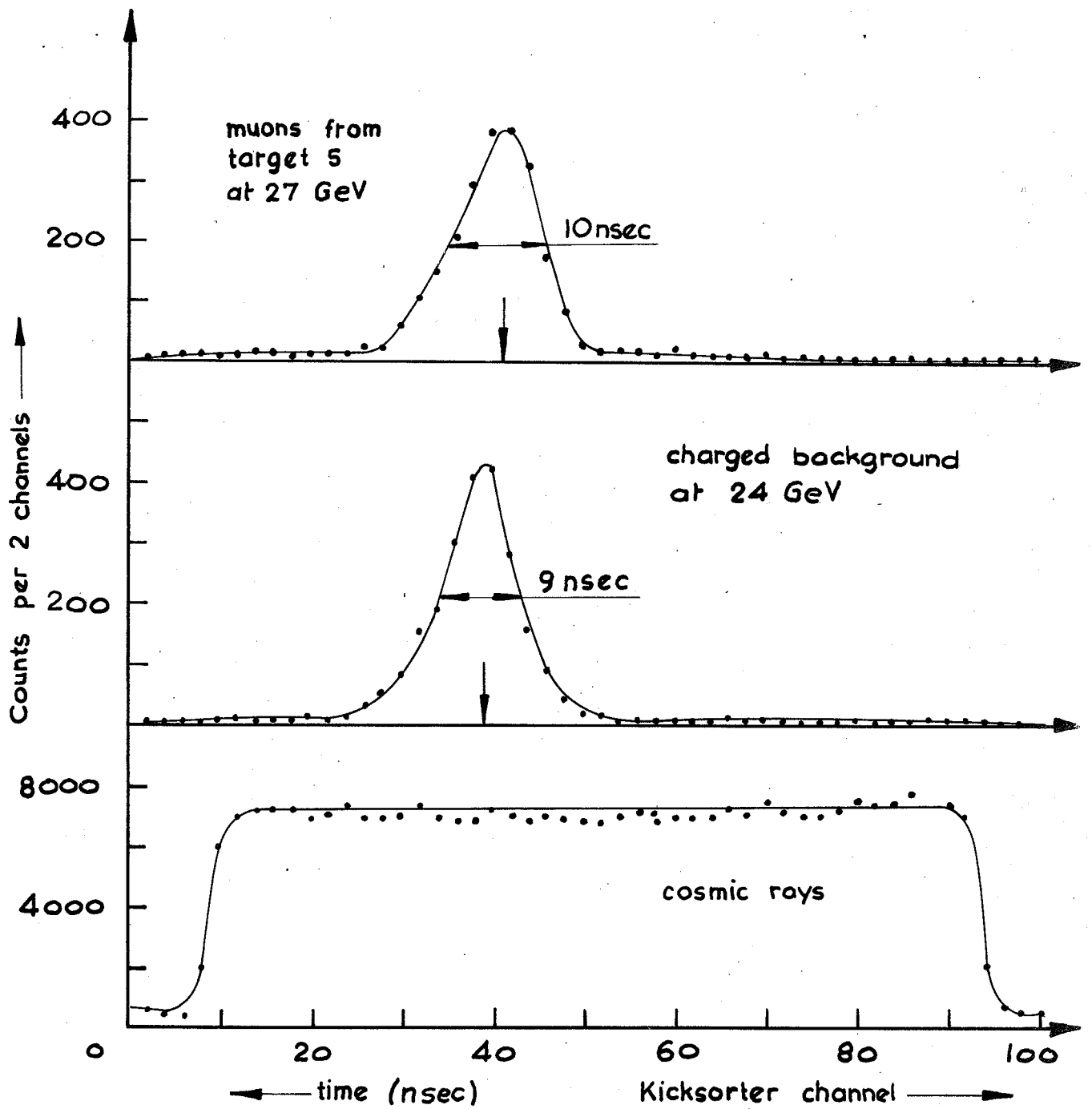


Fig.1

TIME-OF-FLIGHT SPECTRA

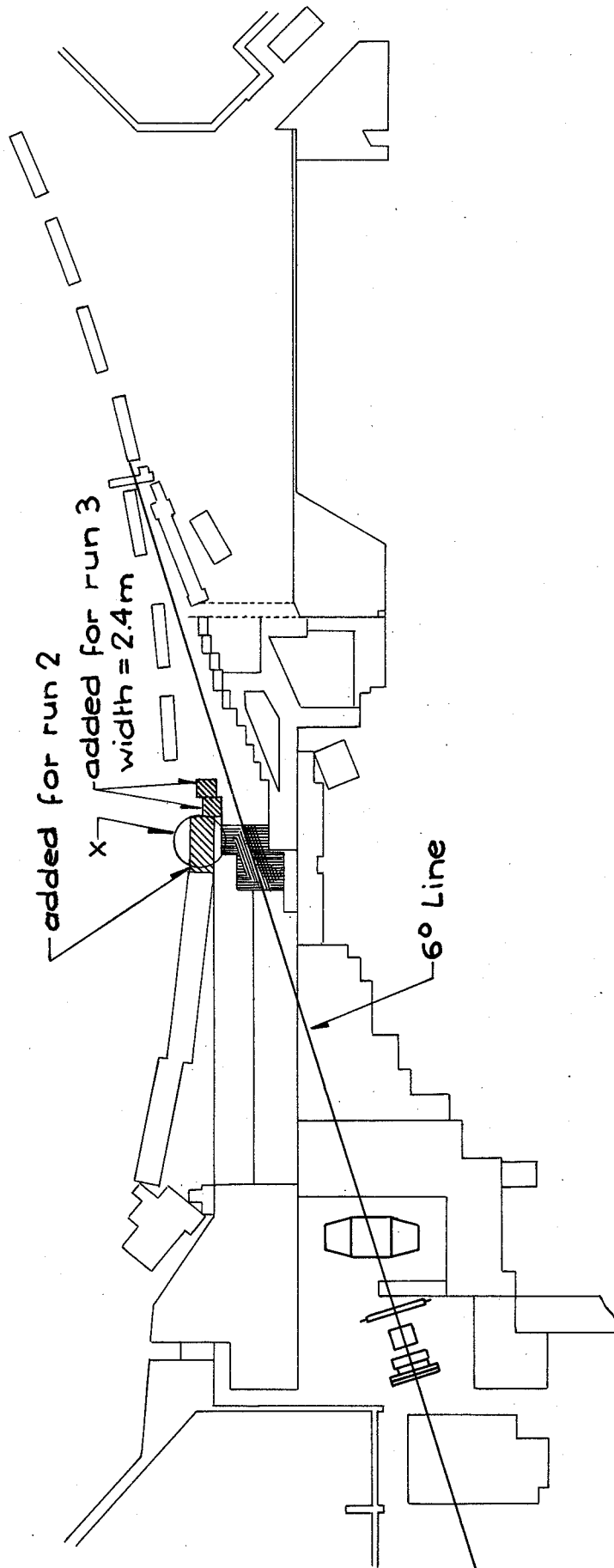


Fig. 2      SHIELDING LAY OUT.



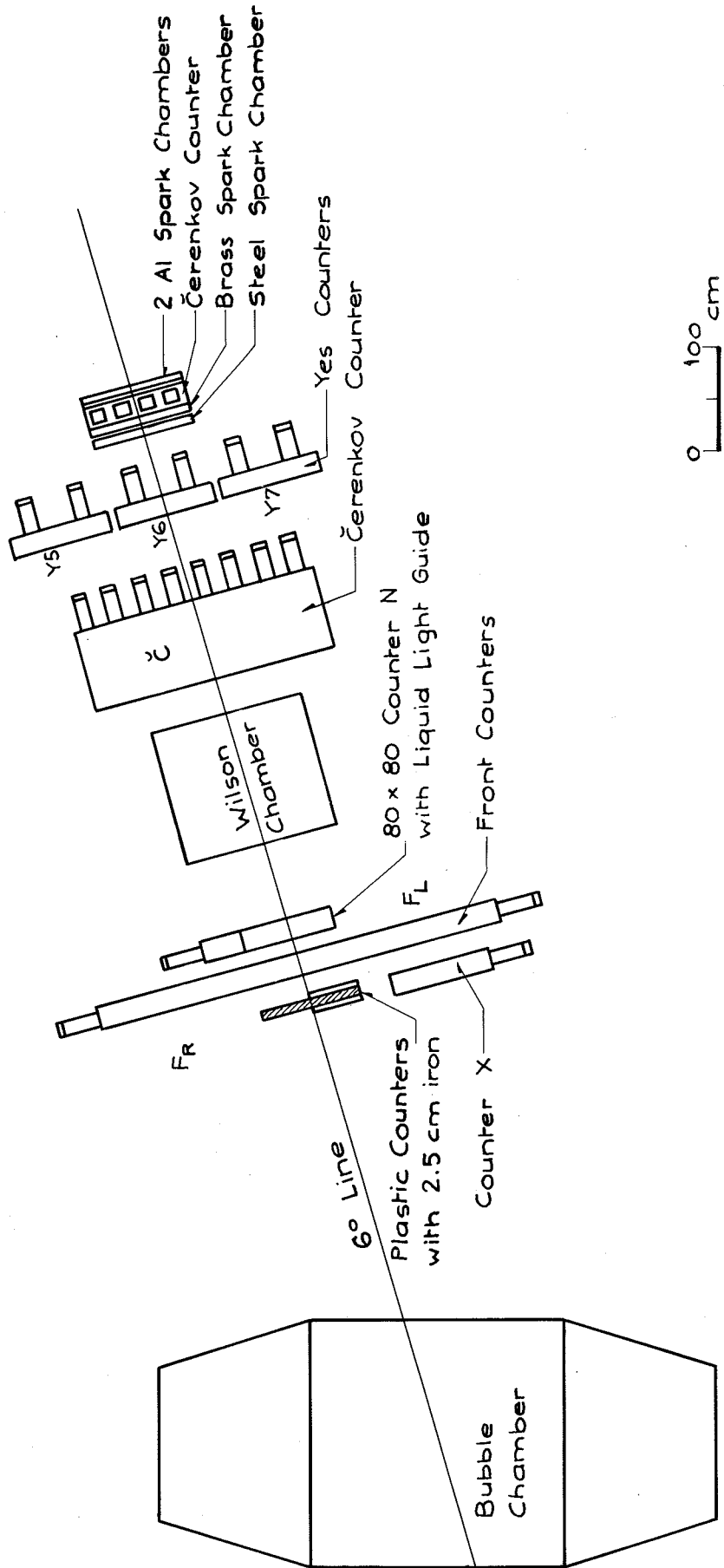
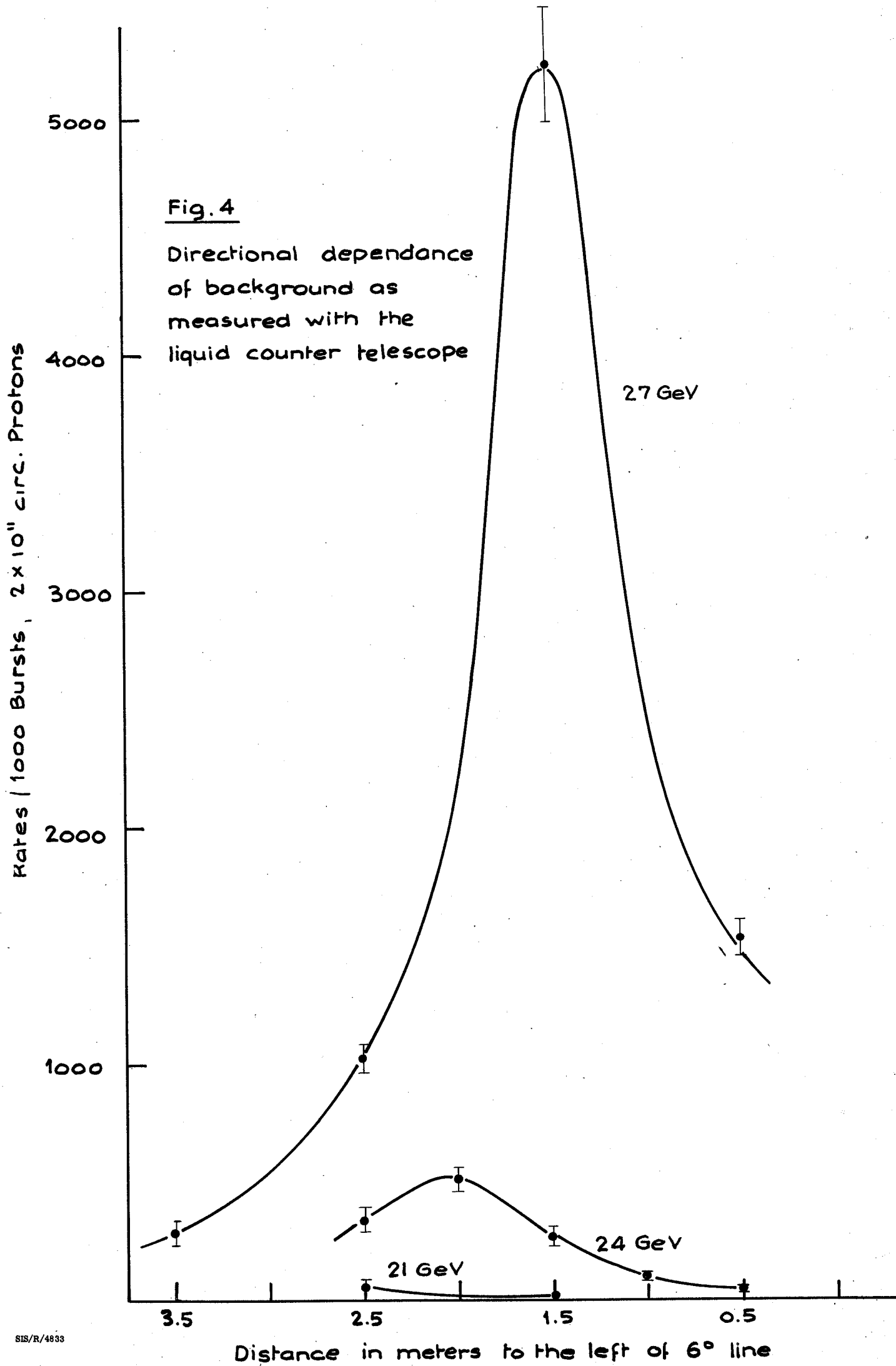


FIG. 3 COUNTER SET UP IN THE NEUTRINO BLOCKHOUSE



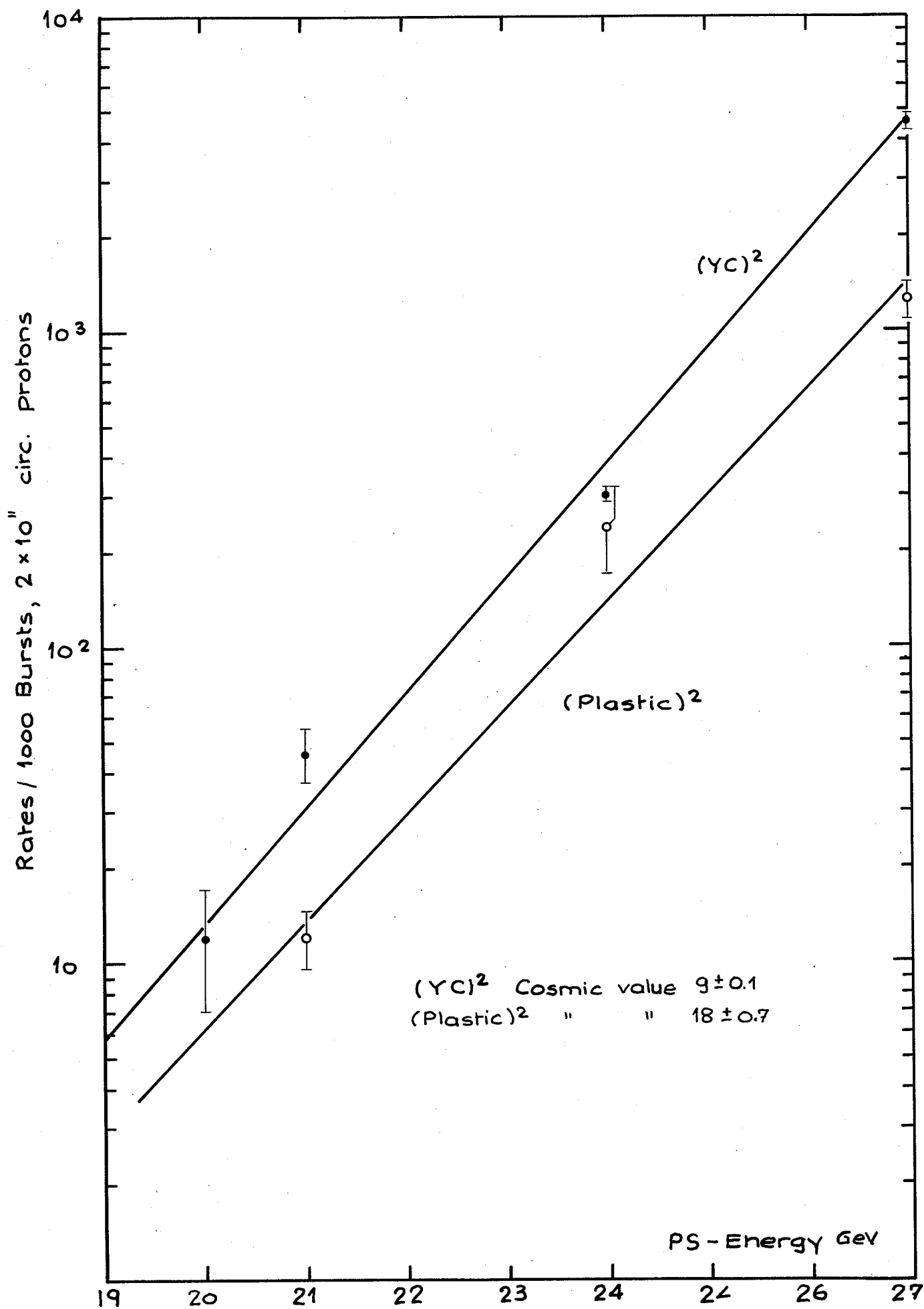


Fig. 5 ENERGY - DEPENDANCE OF  $\mu$ -FLUX.

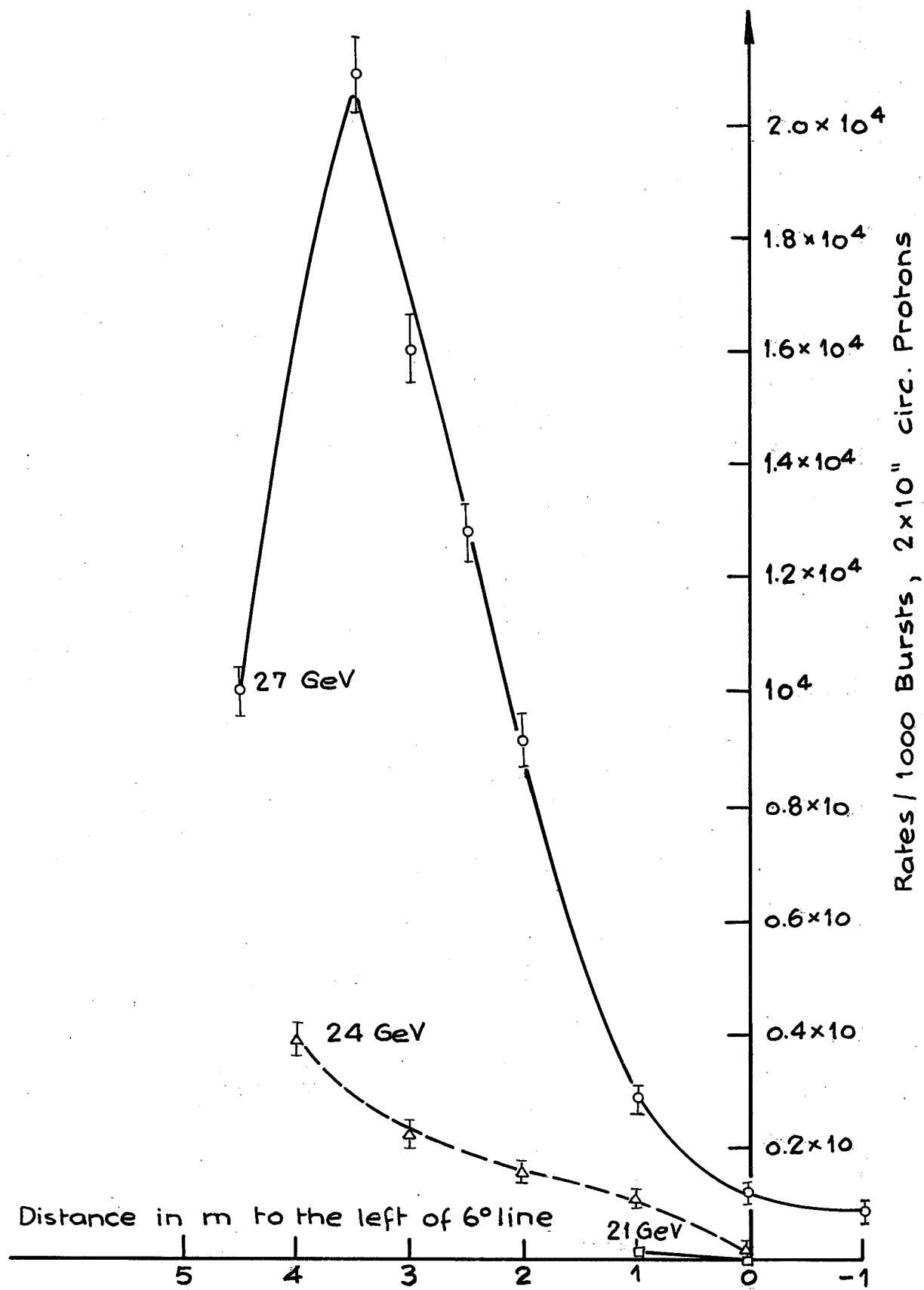


Fig.6

LATERAL DEPENDANCE OF BACKGROUND AS MEASURED WITH PLASTIC COUNTERS.